

## Supporting Information

### Effects of Atomic Geometry and Electronic Structure of Platinum Surfaces on Molecular Adsorbates Studied by Gap-Mode SERS

Jian Hu,<sup>1,2</sup> Masahiro Tanabe,<sup>1</sup> Jun Sato,<sup>1</sup> Kohei Uosaki,<sup>2,3</sup> Katsuyoshi Ikeda,<sup>1,2,4\*</sup>

<sup>1</sup>Division of Chemistry, Graduate School of Science, Hokkaido University, Sapporo 060-0810, Japan.

<sup>2</sup>Global Research Center for Environment and Energy based on Nanomaterials Science (GREEN), National Institute for Materials Science (NIMS), Tsukuba 305-0044, Japan.

<sup>3</sup>International Center for Materials Nanoarchitectonics (WPI-MANA), National Institute for Materials Science (NIMS), Tsukuba 305-0044, Japan.

<sup>4</sup>Japan Science and Technology Agency, PRESTO, 4-1-8 Honcho, Kawaguchi, Saitama 332-0012, Japan.

## DFT simulation of Raman spectra of CPI on Pt

Figure S1a shows the simulated Raman spectra of CPI adsorption on Pt substrates by DFT calculation. The DFT calculation was conducted using GAUSSIAN 09 Revision A02 at the B3PW91 level of theory with LanL2DZ basis set for Pt atom and 6-31G\*\* basis sets for other atoms. The (Pt)<sub>3</sub> cluster was used in the calculations as a model of Pt substrate. Three typical adsorption geometries, i.e., one-fold atop, two-fold bridge, and three-fold hollow configurations, present the corresponding characteristic vibrations of  $\nu\text{NC}_{\text{Pt}}$  at 2132 cm<sup>-1</sup>, 1921 cm<sup>-1</sup>, and 1573 cm<sup>-1</sup>, respectively. The motion vectors for  $\nu\text{NC}_{\text{Pt}}$  corresponding to these three adsorption configurations are shown in Figure S1b. With the increase in the coordination number of NC group, the  $\nu\text{NC}_{\text{Pt}}$  shifts to the lower wavenumber. For the hollow adsorption,  $\nu\text{NC}_{\text{Pt}}$  couples with  $\nu\text{C}=\text{C}(\text{ring})$  in a notable bent configuration, while the other two configurations show the straight configuration.

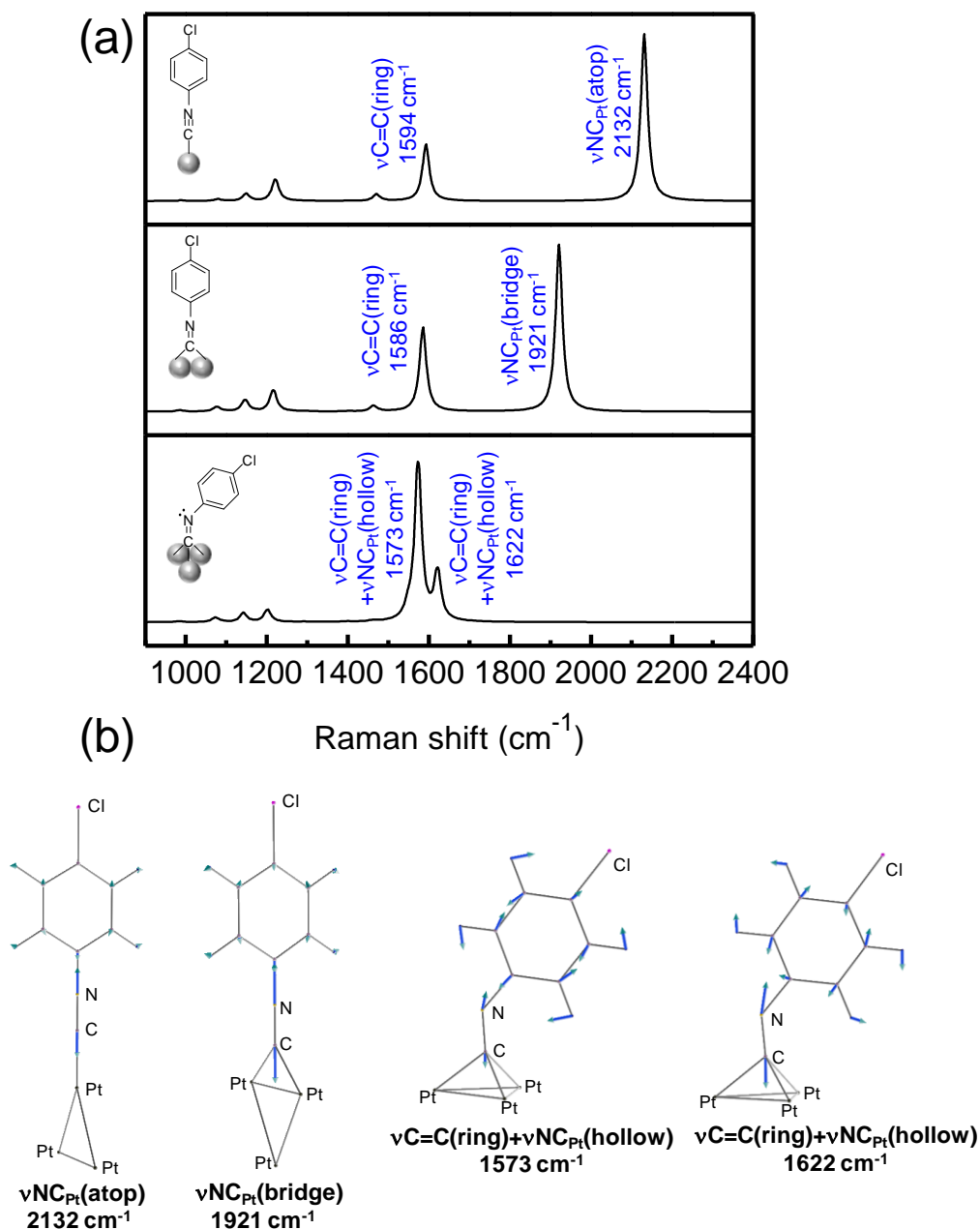


Figure S1. (a) Simulated Raman spectra of CPI adsorption on Pt substrates by DFT calculation. The panels from top to bottom correspond to one-fold atop, two-fold bridge, and three-fold hollow configuration of CPI, respectively. The hollow adsorption exhibits a notable bent configuration while the others a straight configuration. (b) Motion vectors for  $\nu\text{NC}_{\text{Pt}}$  vibrations corresponding to the atop, bridge, and hollow configurations. The peaks at 1573 and 1622 cm<sup>-1</sup> are attributed to the asymmetric and symmetric coupling vibrations between the benzene ring and the NC group for the hollow configuration.

## Pt monolayer formation on Au(111)

As shown in Figure S2a, the Cu underpotential deposition (UPD) on Au(111) is a two-step deposition process, including the first deposition peak (+0.25 V, 147  $\mu\text{C}/\text{cm}^2$ ) and the second deposition peak (+0.09 V, 128  $\mu\text{C}/\text{cm}^2$ ). The splitting of the second deposition peak is the result of two different nucleation processes, one taking place on surface defects and the other on well-ordered (111) terraces. For a two-electron reaction, the coulometric charge of 446  $\mu\text{C}/\text{cm}^2$  would be necessary for the deposition of a fully discharged monolayer of Cu. However, the experimentally obtained charge was 275  $\mu\text{C}/\text{cm}^2$ , indicating the coverage of Cu ( $\Theta_{\text{Cu}}$ ) is 62%. After redox replacement of the Cu monolayer by Pt, a Pt monolayer was formed on Au(111) ( $\text{Pt}_{\text{ML}}/\text{Au}(111)$ ). As shown in Figure S2b, the cyclic voltammogram of  $\text{Pt}_{\text{ML}}/\text{Au}(111)$  shows a Pt-characteristic hydrogen UPD region, indicating the successful deposition of Pt monolayer on Au(111). According to the reduction peak of Pt oxide,  $\Theta_{\text{Pt}}$  was calculated as 69%, quite close to  $\Theta_{\text{Cu}}$ , which indicates the stoichiometric exchange between  $\text{Pt}^{2+}$  and Cu. In addition, the remarkable oxidation and reduction peaks of Au are also observed due to the presence of Au pinholes on the  $\text{Pt}_{\text{ML}}/\text{Au}(111)$  surface.

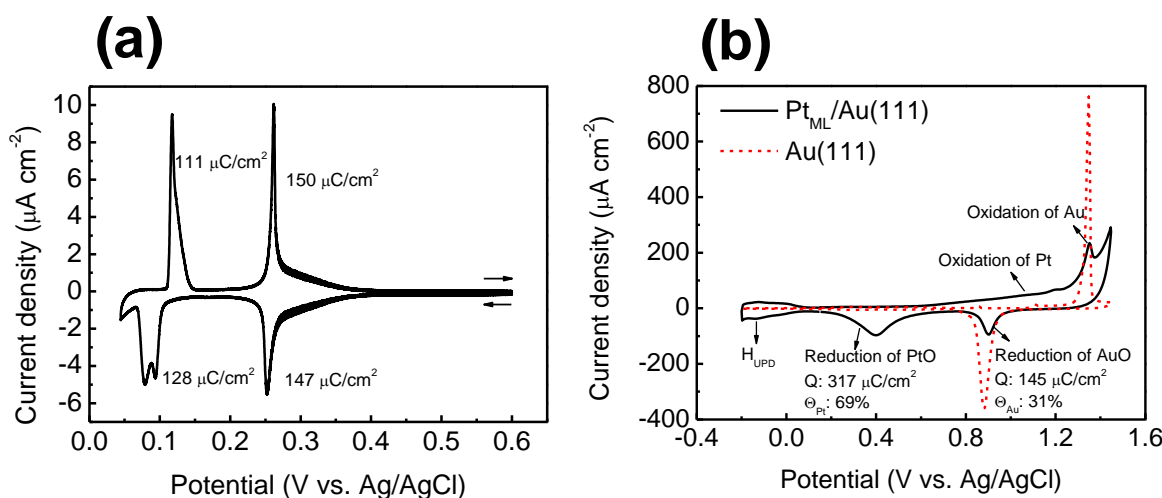


Figure S2. (a) Cyclic voltammogram for Au(111) in 0.1 M H<sub>2</sub>SO<sub>4</sub> + 1 mM CuSO<sub>4</sub>. Scan rate: 1 mV/s. (b) Cyclic voltammograms for  $\text{Pt}_{\text{ML}}/\text{Au}(111)$  and Au(111) in 0.1 M H<sub>2</sub>SO<sub>4</sub>. Scan rate: 50 mV/s.

## Peak assignment for the extramolecular vibrational modes $\nu_{\text{NC-Pt}}$

The preferential adsorption geometry of CPI has been determined to be the hollow on Pt(111) and the atop on Pt(110), according to the intramolecular  $\nu_{\text{NC-Pt}}$ . The corresponding extramolecular  $\nu_{\text{NC-Pt(hollow)}}$  and  $\nu_{\text{NC-Pt(atop)}}$  appear at  $436\text{ cm}^{-1}$  and  $412\text{ cm}^{-1}$  for Pt(111) and Pt(110), respectively, as shown in Figure S3. These results are well consistent with the DFT calculated values, that  $\nu_{\text{NC-Pt(hollow)}}$  and  $\nu_{\text{NC-Pt(atop)}}$  are at  $437\text{ cm}^{-1}$  and  $423\text{ cm}^{-1}$ , respectively.

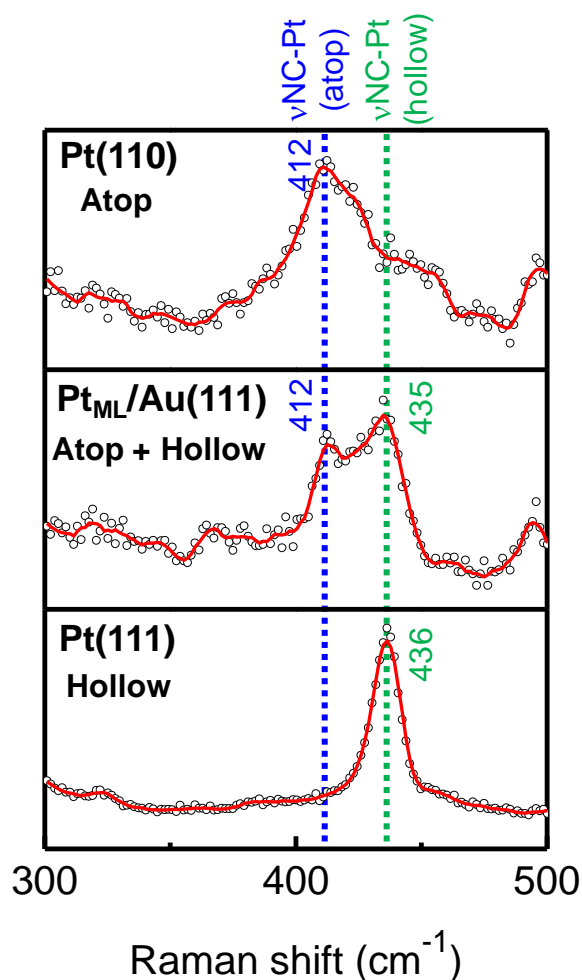


Figure S3. Gap-mode SERS spectra of CPI on Pt(110), Pt<sub>ML</sub>/Au(111), and Pt(111) in the low frequency region.